

Occupancy-based demand response and thermal comfort optimization in microgrids with renewable energy sources and energy storage

Korkas, C; Baldi, S; Michailidis, I; Kosmatopoulos, EB

DOI

[10.1016/j.apenergy.2015.10.140](https://doi.org/10.1016/j.apenergy.2015.10.140)

Publication date

2016

Document Version

Accepted author manuscript

Published in

Applied Energy

Citation (APA)

Korkas, C., Baldi, S., Michailidis, I., & Kosmatopoulos, EB. (2016). Occupancy-based demand response and thermal comfort optimization in microgrids with renewable energy sources and energy storage. *Applied Energy*, 163, 93-104. <https://doi.org/10.1016/j.apenergy.2015.10.140>

Important note

To cite this publication, please use the final published version (if applicable).
Please check the document version above.

Copyright

Other than for strictly personal use, it is not permitted to download, forward or distribute the text or part of it, without the consent of the author(s) and/or copyright holder(s), unless the work is under an open content license such as Creative Commons.

Takedown policy

Please contact us and provide details if you believe this document breaches copyrights.
We will remove access to the work immediately and investigate your claim.

Occupancy-based Demand Response and Thermal Comfort Optimization in Microgrids with Renewable Energy Sources and Energy Storage

Christos D. Korkas^{a,c,*}, Simone Baldi^b, Iakovos Michailidis^{a,c}, Elias B. Kosmatopoulos^{a,c}

^a Dept. of Electrical and Computer Engineering, Democritus University of Thrace, Xanthi 67100, Greece

^b Delft Center for Systems and Control, Delft University of Technology, Delft 2628CD, The Netherlands

^c Informatics & Telematics Institute, Center for Research and Technology Hellas (ITI-CERTH), Thessaloniki 57001, Greece

Abstract

Integration of renewable energy sources in microgrids can be achieved via demand response programs, which change the electric usage in response to changes in the availability and price of electricity over time. This paper presents a novel control algorithm for joint demand response management and thermal comfort optimization in microgrids equipped with renewable energy sources and energy storage units. The proposed work aims at covering two main gaps in current state-of-the-art demand response programs. The first gap is integrating the objective of matching energy generation and consumption with the occupant behavior and with the objective of guaranteeing thermal comfort of the occupants. The second gap is developing a scalable and robust demand response program. Large-scale nature of the optimization problem and robustness are achieved via a two-level supervisory closed-loop feedback strategy: at the lower level, each building of the microgrid employs a local closed-loop feedback controller that processes only local measurements; at the upper level, a centralized unit supervises and updates the local controllers with the aim of minimizing the aggregate energy cost and thermal discomfort of the microgrid. The effectiveness of the proposed method is validated in a microgrid composed of three buildings, a photovoltaic array, a wind turbine, and an energy storage unit. Comparisons with alternative demand response strategies reveal that the proposed strategy efficiently integrates the renewable sources; energy costs are reduced and at the same time thermal comfort of the occupants is guaranteed. Furthermore, robustness is proved via consistent improvements achieved under heterogeneous conditions (different occupancy schedules and different weather conditions).

Keywords: Demand response, Microgrid, Thermal comfort optimization, Occupancy information

1. Introduction

Increasing energy demand and stricter environmental regulations are promoting the transition from traditional electric grids with centralized power plants to smart electrical microgrids where the existing power grid is enhanced by distributed, small-scale, renewable-energy generation systems such as photovoltaic panels, wind turbines, and energy storage units [1]. Microgrids can be seen as miniature versions of the larger utility grid except that, when necessary, they can disconnect from the main grid and can continue to operate in ‘islanded mode’ [2]. Despite their potential advantages, a main challenge needs to be overcome: the

*Corresponding author. Tel.: +30 2541 551597

Email addresses: ckorkas@ee.duth.gr (Christos D. Korkas), s.baldi@tudelft.nl (Simone Baldi), michailid@iti.gr (Iakovos Michailidis), kosmatop@iti.gr (Elias B. Kosmatopoulos)

widespread availability of renewable sources inserts uncertainty into the grid, due to their stochastic output profile which strongly depends on local weather conditions. Lack of monitoring and control of these energy sources might contribute to the instability of the electric grid: this is especially true in grids where fluctuating power may be delivered due to the high participation of renewable energy sources [3]. Energy storage systems play a central role in the integration of renewable energy sources in microgrids, as they provide the necessary flexibility to compensate unbalances between the power supply and the demand. The interesting experimental work in [4] assesses how the timing of an electric outage affects the islanding lifetime of a microgrid, with and without energy storage. For these reasons, one of the pivotal questions in the widespread diffusion of microgrids is to deploy a control system which will take the appropriate decisions for the energy distribution and consumption, in order to minimize the energy consumption and cost: this task goes under the name of ‘demand response’ [5].

Demand response requires the development of control mechanisms that can autonomously facilitate changes in electric usage by end-use customers in response to changes in the price of electricity over time, or in response to the availability of renewable energy [6]. The implementation of these mechanisms require the presence of loads whose operation can be regulated, i.e. controllable loads. Many studies show that HVAC operations account for nearly 50% of the energy consumed by a building [7]: furthermore, good HVAC control is one of the most cost-effective option to implement demand response and improve the energy efficiency of microgrids. For example, it has been shown that raising summer set point temperature might have good and universal energy saving potential as it can be applied to both new and existing buildings [8]. However, HVAC operation cannot aim exclusively at energy savings without taking into account the effect of changing the control strategy on indoor comfort: the ASHRAE55 and EN15251 standards [9, 10] pose strict constraints on the end-user (building occupant) thermal comfort, with bounds and constraints that should not be violated except for small intervals during the building operation. The literature on demand response with thermal comfort optimization is vast: without aiming at being comprehensive, in the following we give a brief overview on the topic.

1.1. State-of-the-art in demand response with thermal comfort

As a large portion of building energy consumption is used for thermal comfort, optimization of energy and comfort calls for delicate trade-offs, which have been studied by many researchers: the simulation tool of [11] can predict the effect of changing the control strategy on indoor comfort and energy consumption. The authors of [12] develop control strategies for intelligent glazed facades and investigate the influence of different control strategies on energy and comfort performance in office buildings. Particle swarm optimization has been applied in [13] to optimize the set points based on the comfort zone. In [14] the operation of variable air volume air conditioning is optimized with respect to comfort and indoor air quality. The influence on energy consumption of thermostat operation and thermal comfort requirements is the object of the study in [15]. All this approaches show, sometimes also via real-life experiments, that relevant energy savings can be achieved without compromising thermal comfort.

The use of occupancy information plays a major role in decreasing energy costs and improving thermal comfort: the potential of using occupancy information in model predictive-based building climate control is investigated in [16]. The approach of [17] aligns the distribution of residents’ thermostat preferences with the indoor temperature to maximize thermal comfort while reducing energy savings. Using the expected room occupancy schedule, the evolutionary algorithm of [18] produces optimized ventilation strategies with reduced CO₂ concentration and energy costs. The goal of [19] is to use occupancy information to reduce energy use while maintaining thermal comfort and indoor air quality.

Multi-objective optimization of energy consumption and thermal comfort is well established at the building level: at the microgrid level, however, most state-of-the-art microgrid energy management systems

aiming at improving resilience and enabling islanded mode, consider only matching energy generation and consumption [20, 21, 22]: other multi-objective optimization examples include optimize the power dispatch of the microgrid according to economy and reliability interests of the power grid [23], decreasing the expenses for power purchase or increasing revenues from power selling [24]. Operational results of real-life microgrids have also been provided [25, 26, 27]. However, in the aforementioned works and experimental evaluations, thermal comfort of the occupants is often neglected, or, when considered, it is oversimplified. A typical oversimplification involves considering bounds on the dry-bulb temperature [28]: this is a poor comfort-maintaining criterion, since neglecting humidity and radiant temperatures can lead to insufficient estimation of actual thermal comfort. The Fanger index [9] or adaptive thermal comfort models [29] can yield a realistic estimate of thermal comfort. Summarizing, to the best of the authors' knowledge the following gaps can be identified in the state of the art of demand response in microgrids:

- G1) *Thermal and occupancy information in microgrids*: a part from some recent contributions by the authors [30], there is no demand response program at the microgrid level that can exploit occupancy information with the objective of guaranteeing thermal comfort of the occupants. Note that the work in [30] do not consider the presence of multiple renewable energy sources (possibly with different prices) and of energy storage.
- G2) *Scalability to large microgrids*: there is no demand response program that can be scalable to large-scale microgrids: also the recent work in [19] considers a centralized architecture stemming information from the entire microgrid: this might be impractical in microgrids of large dimension.
- G3) *Robustness of solution*: there is no real study on robustness of demand response programs in front of changing conditions, including changing occupancy patterns and changing weather conditions: due to the computational complexity of predictive control strategies, most of the cited state-of-the-art demand response are tested over relatively short horizons, and it is not clear whether they can achieve consistent improvements over longer ones. Furthermore, their predictive control nature requires the optimization task to be continuously active: it is not clear whether it is possible to develop a demand response program that, after optimization over a short horizon, can be used over longer horizons with consistent improvements.

With this work we try to cover the identified gaps in demand response and thermal comfort optimization in microgrids, as explained hereafter.

1.2. Main contributions of the work

This paper presents a novel control algorithm for joint demand response management and thermal comfort optimization in microgrids equipped with renewable energy sources and energy storage. With respect to the three identified gaps, the work provides the following contributions:

- C1) *Thermal and occupancy information in microgrids*: demand response is achieved by controlling the HVAC system of each building: the final objective is not only the reduction of the energy absorbed from the traditional electrical grid, but also guaranteeing acceptable thermal comfort conditions. The Fanger index is used as a realistic measure for thermal comfort. The proposed system uses a simulation-based optimization procedure: together with Model Predictive Control (MPC) [31, 32, 33, 34], simulation-based optimization is emerging as a strategy for energy-efficient control and smart grids [35, 36, 37, 38]. The proposed demand response program is a parametrized feedback control strategy where the parameters are dependent on the thermal state of the buildings, but also on the occupancy pattern of the microgrid : this will lead to efficient exploitation of the occupancy information stemming from the microgrid.

C2) *Scalability to large microgrids*: from the control perspective, a microgrid is a large-scale dynamic system with high complexity and a huge amount of information. Proper combination of the available information and effective control of the overall microgrid system turns out to be a big challenge [39]. In order to address the computational complexity, the proposed control strategy adopt a two-level supervisory strategy: at the lower level, each building employs a local controller that processes only local measurements; at the upper level, a centralized unit supervises and updates the three controllers with the aim of minimizing the aggregate energy cost and thermal discomfort of the microgrid. This distributed architecture is supposed to be scalable to microgrids composed of many buildings.

C3) *Robustness of solution*: simulation-based optimization allows the use of elaborate microgrid models (built via simulation tools like EnergyPlus, TRNSYS, Modelica etc. [40, 41]): an advantage is that reliable simulations over long horizons can be conducted in order to address the large-scale complexity and the real-time requirements. The parametrized demand response strategy developed in this work will be used to test to what extent a demand response program optimized over short horizons can be robust when implemented over long horizons: it will be verified that the proposed demand response program, due to its feedback nature employing thermal and occupancy information, achieves consistent improvements in front of changing conditions, including changing occupancy patterns and changing weather conditions. This is a relevant achievement in terms of required computational complexity, as it shows that optimization does not have to be carried out continuously but, after optimization over a short horizon, the proposed demand response program can be used over longer horizons with consistent improvements.

A test case consisting of a microgrid with three buildings connected to a photovoltaic array, a wind turbine, an energy storage and to the traditional electrical grid is used to evaluate the effectiveness of the proposed algorithm. Comparisons with alternative demand response strategies reveal that the proposed supervisory strategy efficiently handles the large-scale of the optimization problem, manages the demand response so as to sensibly improve independence of the microgrid with respect to the main grid, and guarantees at the same time thermal comfort of the occupants.

The paper is organized as follows: Section II describes the problem setting, the microgrid and its attributes. Section III deals with the control objectives and the performance index. In Section IV the supervisory control architecture is presented, while Section V presents the PCAO algorithm used for the optimization problem. Section VI presents the results and Section VII concludes the paper.

2. Problem description

In this section we present the setting of the joint demand response management and thermal comfort optimization problem. A grid-connected microgrid, shown in Figure 1, is composed of three buildings and equipped with renewable energy sources (photovoltaic panels and wind turbines) and a shared energy storage unit for electricity. The grid is also connected to the main electricity grid. In order to fulfill their energy needs, the buildings of the microgrid share the energy sources and the stored energy in a common pool: the renewable energy sources are so-called ‘must-take’ sources, where their output is always used when it is available. If the output of the renewable energy sources is not enough, the extra electricity is absorbed for the main grid. In the following, more details about the different components of the microgrid are given.

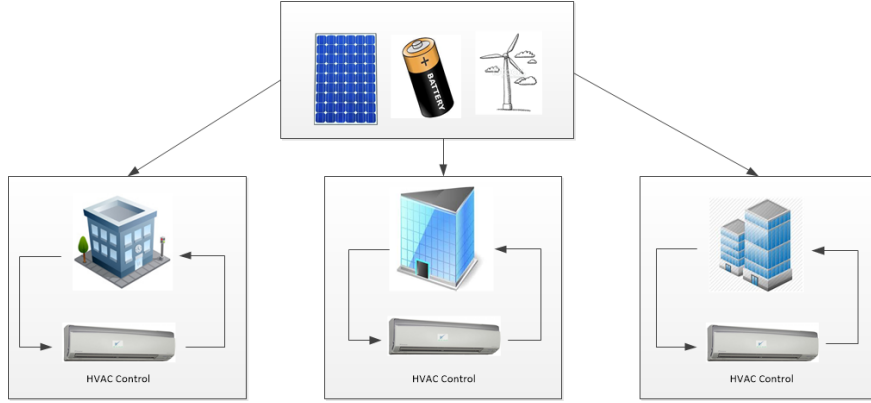


Figure 1: Supervisory Control Strategy

Table 1: Microgrid description

	No. of Thermal Zones	Size	Use
Building 1	10 thermal zones	500 m^2	Industrial
Building 2	10 thermal zones	900 m^2	Commercial
Building 3	10 thermal zones	300 m^2	Residential

2.1. Controllable and uncontrollable loads

Table 1 shows the composition of the microgrid: the three buildings cover a surface of 500 m^2 , 900 m^2 and 300 m^2 , respectively. In order to consider a heterogeneous microgrid scenario with different occupancy patterns, we assume that the buildings are of commercial, industrial and residential type, respectively. Each building has two floors and ten thermal zones. Each thermal zone is equipped with an HVAC unit, where every HVAC unit is opportunely dimensioned according to the size of the thermal zone. This results in a scenario where each building has different energetic needs. The HVAC are operated via temperature set points, one for each unit: by regulating the thirty set points, part of the energy demand of the microgrid is controlled. In our setting HVACs are the only controllable loads of the microgrid: this is based on the fact that HVAC operation accounts for nearly 50% of the energy consumed by a building and on the hypothesis that the other types of loads of the microgrid (lighting, industrial machines, PCs, etc.) are not responsive and cannot be curtailed [42]. Uncontrollable loads account for the not responsive part of the energy consumption: three load daily profiles, shown in Figure 2 have been created based on typical profiles of commercial, industrial and residential consumers [43, 44, 45].

2.2. Occupancy schedule

In order to make the joint demand response and thermal comfort optimization tasks more challenging, the three buildings are assumed to have different occupancy schedules, which are shown in Table 2. Roughly speaking, when the three buildings of the microgrid have a different occupancy schedule, the demand response program should be able to switch off the HVACs of a building when no occupants are there, in order to allow the other buildings to use the available renewable energy. The different occupancy schedules arise from the different use of each building. In particular, the first building is assumed to host industrial activities and the second building is used as an office; the third building exhibits a possible residential occupancy

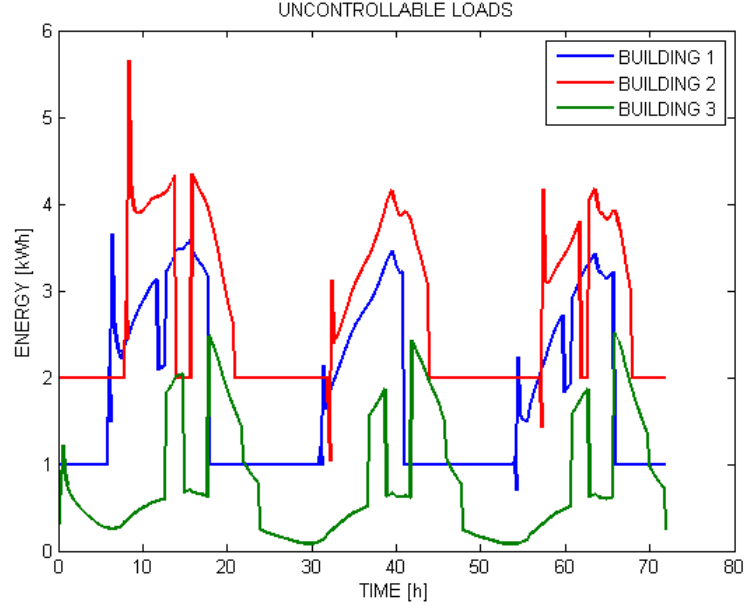


Figure 2: Uncontrollable loads of the three buildings over three days

183 schedule. The schedule of Table 2 has been designed in such a way that a variety of situations occur. Some-
 184 times all three buildings are occupied and, other times, only one building is occupied. It is assumed that all
 185 the thermal zones of a building exhibit the same occupancy pattern.

Table 2: Occupancy Schedule

	Day 1	Day 2	Day 3
Building 1	6am - 12am and 13pm - 18pm	7am - 17pm	6am - 12am and 13pm - 18pm
Building 2	8am - 14pm and 16pm - 21pm	8am - 20pm	9am - 14pm and 15pm - 20pm
Building 3	0am - 24pm	0am - 24pm	0am - 24pm

186 2.3. Renewable energy sources

187 The energy from the renewable sources comes with a different price, as shown in Table 3: the different
 188 prices account for the fact that producing solar energy costs differently than producing wind energy [46, 47].
 189 Furthermore, the prices of the electricity generated by renewable energy includes also investment costs and
 190 maintenance costs of resources [48]. Because of the different prices, the energy is absorbed in the following
 191 order: wind, solar, storage, main grid. The energy is drained proportionally to the energy demand of each
 192 building of the microgrid according to the Kirchhoff's circuit law.

193 The amount of photovoltaic generation P_s is calculated via the model described in [49]

$$P_s = \eta S I_a (1 - 0.005(T_{amb} - 25)) \quad [kWh] \quad (1)$$

194 where η is the conversion efficiency of photovoltaic array (%), S is the array area (m^2), I_a is the solar
 195 radiation (kW/m^2), T_{amb} is the outside air temperature ($^{\circ}C$). It is assumed that the total radiation is falling

Table 3: Energy prices

	Grid Energy	Solar Energy	Wind Energy
Price	0.2 €/kWh	0.1 €/kWh	0.05 €/kWh

on the photovoltaic array, and the angle of incidence is not considered. Conversion efficiency η is equal with 20% which is a typical value for solar arrays and the array area S is equal with 200 m^2 . The wind turbine produces energy P_M based on the following equation [50]:

$$P_M = 1/2 \rho \pi R^2 V^3 C_P(\lambda, \beta) \quad [\text{kWh}] \quad (2)$$

where V is wind speed in $[\text{m/s}]$, ρ is the air density in $[\text{kg/m}^3]$, R is the blades radius in $[\text{m}]$ and C_P the power coefficient. We assume $\rho = 1.1839 \text{ kg/m}^3$, the air density at sea level and 25°C , $R = 20 \text{ m}$, and a constant $C_P = 0.4$, which are the typical values for wind turbines.

Finally, the microgrid is equipped with a battery as energy storage: the battery is charged when there is excess of energy coming from the renewable resources and discharged when the energy coming from the renewable resources is not enough to satisfy the energy demand of the microgrid [51]. The capacity of the battery unit is set to 200 kWh . However, only 150 out of 200 kWh are available for use. That is because, we want to avoid discharge greater than 10 % and charge greater than 85 % in order to prologue the life of the battery. Thus, in Figure 8, the state of charge of the battery for each scenario is between 10 and 85 %. What is more, the rate of charge/discharge was also investigated. Using a 1C charger, and taking into account that our battery has a capacity of 200 kWh , our system has a capability of charge/discharge rate of 200 kW . However, in Figure 8, the mean rate of charge between the scenarios is around 35 kW and the mean rate of discharge is around 40 kW . Just once, a peak of 174 kW charge rate is developed, but the battery system is able to handle it, without wasting any amount energy.

The attractiveness of utility-scale energy storage is that it can compensate for the intermittency of wind power and solar power. It must be however underlined that in practice large-scale storage technologies other than pumped hydro remain in an early stage of development and are expensive [52, 53].

3. Control objectives

One objective of the demand response program is to reduce energy costs: this is achieved if the energy available from the renewable sources, which indirectly affects also the energy stored in the storage unit, is exploited to the maximum extent. The problem is not trivial since the renewable energy is available depending on weather conditions. The wind and solar energy over three different days, depending on wind speed and solar radiation respectively, are shown in Figure 3. When the sum of renewable energy and stored energy is not enough, extra energy can be absorbed from the main grid. On the other hand, if the energy that the renewable sources produce is in excess compared to microgrid energetic needs, the energy is stored in the battery; if the storage is at its maximum capacity, the excess of energy is wasted. It is crucial to fully take advantage of renewable energy when available in order to enable the ‘islanded mode’ of the microgrid and minimize the dependence from the main grid. The demand response is regulated by regulating the HVAC operation: the HVAC operation has a direct impact not only on energy demand, but also on the thermal comfort of the occupants. If one objective of the demand response program is to reduce energy

costs, another objective is to manage the HVAC operation so as to satisfy the thermal comfort of the users. The two objectives are expressed by a suitable performance index as explained hereafter.

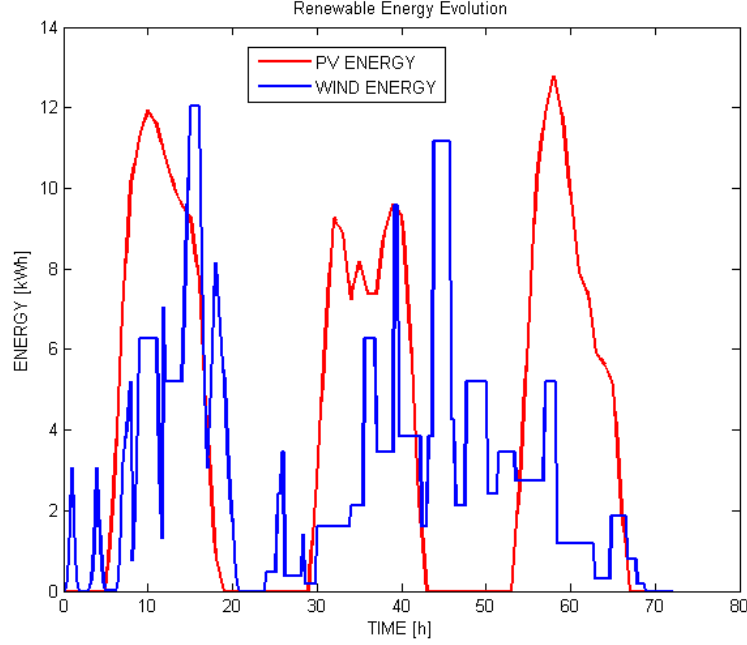


Figure 3: Solar and wind energy evolution over three days

3.1. Performance Index

The performance index to be optimized takes into account two terms: the energy cost and the thermal comfort of the occupants. At time t the aggregate performance index of the three-building microgrid is defined as

$$M(t) = \sum_{i=1}^3 (k * E_i(t) + (1 - k) * C_i(t)) \quad (3)$$

where E_i is the energy score and C_i the thermal comfort score of building $\#i$. The energy and the comfort score are, typically scaled, so as to be of the same order of magnitude and contribute fairly to the total score. According to the importance that the designer wants to give to a term with respect to the other, the summation can be weighted using the scaling factor $0 < k < 1$.

The energy cost includes the price paid for absorbing energy from the main grid, but also the generation/maintenance price of renewable energy. The thermal comfort cost we consider is the thermal comfort model developed by Fanger [9], which evaluates the Predicted Percentage of Dissatisfied people (PPD) in a room. According to the condition of a thermal zone, the thermal comfort is evaluated via a 7-point scale, going from -3 (cold) through 0 (neutral) to +3 (hot). Such a scale is called Predictive Mean Vote (PMV). The PMV is translated into PPD according to the following formula

$$PPD = 100 - 95e^{-(0.03353PMV^4 + 0.2179PMV^2)} \quad (4)$$

According to the ASHRAE 55 standard, the recommended PMV range for thermal comfort is between -0.5 and +0.5 for an interior space, which is equivalent to a PPD below 10%. Violation of this bounds are accepted but only over short periods of time.

3.2. Rule-based demand response programs

An EnergyPlus model [40, 54] simulates the complex energetic and thermal behavior of each building composing the microgrid. The implemented demand response program considers the problem of operating the HVAC during summer, in order to cool-climate the rooms in an energy efficient manner to a user comfort satisfying level. The operation of the each HVAC unit has one manipulable input that is the temperature set point (in $^{\circ}C$) with which each unit operates.

For comparison reasons, two Rule Based Controllers (RBC) implementing simple but common demand response programs are adopted. The RBCs employ a simple control strategy, which consists of

- $RBC_{24^{\circ}C}$: keep the HVAC set points of each thermal zone constant to $24^{\circ}C$ during occupancy hours;
- $RBC_{25^{\circ}C}$: keep the HVAC set points of each thermal zone constant to $25^{\circ}C$ during occupancy hours;

Such control strategies, yet simple, provide acceptable (but far from optimal) performances in terms of the total score (3). Furthermore, in order to exploit natural ventilation and achieve some energy savings, the HVAC set point manipulation of $RBC_{24^{\circ}C}$ and $RBC_{25^{\circ}C}$ is combined with control of windows. Every time that HVAC units operate, windows are closed. When the HVAC unit are switched off, the window control is as follows:

$$\begin{cases} \text{open window} & \text{if } T_{amb} < T_z \text{ and } T_z > 20^{\circ}C \\ \text{close window} & \text{otherwise} \end{cases} \quad (5)$$

where T_{amb} is the outside temperature and T_z the temperature of the thermal zone. Taking into account that we want to cool-climate the buildings, the rule in (5) is meant to exploit the natural ventilation effect occurring typically at night (the room is cooled using the outside temperature). The bound of $20^{\circ}C$ is set in order to guarantee a minimum thermal comfort: if the temperature of the room is already below $20^{\circ}C$ there is no need to open the window.

On the other hand, in order to guarantee the quality of indoor conditions a third window rule is implemented when HVAC are operating. If the internal conditions, and especially the quality of air (big amounts of humidity) are very low, then windows open, so an external air flow help regulate the conditions inside the building. Thus, when the HVAC unit are operating, the window control is as follows :

$$\begin{cases} \text{open window} & \text{if } humidity \geq 80 \% \\ \text{close window} & \text{otherwise} \end{cases} \quad (6)$$

However, it has to be emphasized that the rule in 6 is never activated in our simulations, meaning that the HVAC, is never used by the system, as the HVAC manage to keep internal conditions in acceptable levels during the whole simulation period. *In the setting of this paper interaction between local and aggregate level occurs via the occupancy schedule: the demand response program should be able to switch off the HVACs of a building with no occupants, in order to allow the other buildings to use the available renewable energy.*

In this section we explained how the emphasis of the work is on joint optimization of energy cost and thermal comfort. As the microgrid is composed of three buildings, a distinction should be made between the performance achievable at the building level and the performance achievable at the aggregate level. In the following section the two levels and their interaction are presented.

4. Control Strategy

In this section, we present the control strategy that it is used in the presented microgrid test case. In Figure 5, the general form of Supervisory Control Strategy is described. Each buildings, uses its own

284 optimization algorithm (PCAO) and a general node is responsible for the coordination of the different
 285 buildings.

286 4.1. PCAO Algorithm

287 The problem consists in finding an optimal strategy for the HVAC set points such that the combined
 288 performance index defined in (3) is minimized. The problem is thus formulated as an optimal control
 289 problem aiming at minimizing the index

$$J = \int_0^{T_f} \Pi(x(t))dt \quad (7)$$

s.t.

$$\dot{x} = f(x) + Bu, \quad B = [0 \ I]' \quad (8)$$

290 where $\Pi(\cdot)$ is the analytical expression of the performance index (3), where x is an augmented, with state
 291 and control variables, vector of the transformed system dynamics while u is the time derivative of the actual
 292 control signals, as demonstrated in 8. The function $f(x)$ represents the microgrid dynamics, which are
 293 implemented inside the EnergyPlus model, but that are unknown for our purposes. Finally T_f is a control
 294 horizon over which we have reliable weather forecasts (typically 2-3 days). Using dynamic programming
 295 arguments, we know that the optimal strategy u^* satisfies the Hamilton-Jacobi-Bellman (HJB) equation

$$\frac{\partial V^*}{\partial x} (f(x) + Bu) + \Pi(x) \quad (9)$$

296 The difficulty in solving the HJB equation in large-scale systems (like our microgrid) was known to Bellman
 297 itself, which coined the term ‘curse-of-dimensionality’ [55]: in order to overcome such difficulties, the
 298 PCAO (Parametrized Cognitive Adaptive Optimization) algorithm parametrizes the solution of the HJB
 299 equation (9) as $V^*(x) = z'(x)Pz(x)$ and the optimal control strategy via $u^* = -\frac{1}{2}B'\frac{\partial V^*}{\partial x}$, P is a positive definite
 300 matrix and $z(\cdot)$. More details for the function $z(\cdot)$ can be found in [56, 57]: in our specific microgrid case we
 301 found that a linear transformation $z(x) = x$ is sufficient to achieve important improvements (as demonstrated
 302 in Section V). With such parametrization, the problem of solving the HJB equation is recast as the problem
 303 of finding the matrix P (and thus the strategy u) that better approaches the solution of the HJB equation.
 304 The PCAO algorithm defines the close-to-optimality index (mutated for the principle of optimality [55])

$$\varepsilon(x, P) = V(x(k+1)) - V(x(k)) + \int_k^{k+1} \Pi(x(t))dt \quad (10)$$

305 The solution of the HJB equation (9) brings (10) to zero: the PCAO algorithm, whose steps are presented
 306 in Figure 4 updates at every time step the strategy parametrized by \hat{P} in an attempt to minimize the close-
 307 to-optimality index $\varepsilon(\hat{P})$ and to make \hat{P} converge as close as possible to the solution of the HJB equation.
 308 More about PCAO algorithm can be found in [30, 57, 58]

309 4.2. Feedback vector and Simulation based optimization

310 Each local P-CAO algorithm employs a controller based on a local feedback vectors. The structure of
 311 each local feedback vector is the following:

- 312 • 3 measurable external weather conditions: outside temperature, outside humidity and solar radiation.
- 313 • 6 forecasts for the mean outside temperature in the next 6 hours.

- 6 forecasts for the mean solar radiation over the next 6 hours.
- The n temperatures of the thermal zones (n is the number of thermal zones).
- The n humidities of the thermal zones.
- A constant term (since the equilibrium of the system is not in the origin).
- The n set points of the HVAC devices in the thermal zones.
- The n detectors of occupancy in the thermal zones.

Hereafter we explain with more details the choice of the feedback vector: the zone temperature and humidities are a natural choice for the thermal state of the building; outdoor weather conditions both in the present and the future help to achieve a pro-active control strategy. Finally, the information about the occupancy of a thermal zone is provided as a feedback component to the control strategy. The occupancy signals are important also for another reason. A frequent problem in building management is the creation of comfortable conditions just before people start using the building. In order to achieve this, many control strategy uses a training period to "learn" the occupancy schedule. Many smart thermostats available in the market employ this mechanism: this is a very useful feature, especially for buildings that are used as schools, offices and public offices. Knowing the schedule of occupancy we can change the occupancy signals to "on", one hour before the arrival of users in order to create better thermal comfort conditions for the people.

Using the PCAO algorithm, as presented above, a double feedback loop procedure runs in each building (cf. Fig. 4). The primary feedback loop runs in real-time, with actions applied to the actual building and measurements collected. In parallel with the primary loop, a secondary simulation-based loop interacts with the EnergyPlus model of the building, in order to find better strategies at the next time step. With the term 'simulation-based' design we refer to a method where the optimization of the cost function involves an iterative process of system simulation/controller redesign. At this point is crucial to introduce and explain two time metrics. The control horizon and the simulation horizon. By control horizon we refer to the time interval of HVAC management. For example in our test case, the HVAC set points are changed by the algorithm every 10 minutes. On the other hand, as a simulation horizon we refer to the whole duration of the experiment. Usually, as a simulation horizon we refer to one day or more. This two-loop design is implemented in each building separately. The secondary loop, which is implemented based on the EnergyPlus model, operates in order to find a better controller for the real system. Simultaneously, the primary loop/system, uses the best so-far controller to manage the HVAC. The above two-loop procedure can be investigated better in Figure 4.

Remark 1. *The proposed control strategy differs from the classical rolling (or receding) horizon philosophy. In particular, the objective is to update at every time step a feedback controller, rather than solving at every time step an open loop control problem. After convergence, it was verified via simulations that the proposed feedback solution provides robustness to the resulting HVAC controller, also in the presence of different weather conditions than the one used for the design (cf. the results in Table 4). As a result, simulation results reveal that one can realistically assume keep the same control strategy over long horizons (indicatively, one week) without the need of redesign the control and without sensible loss of performance.*

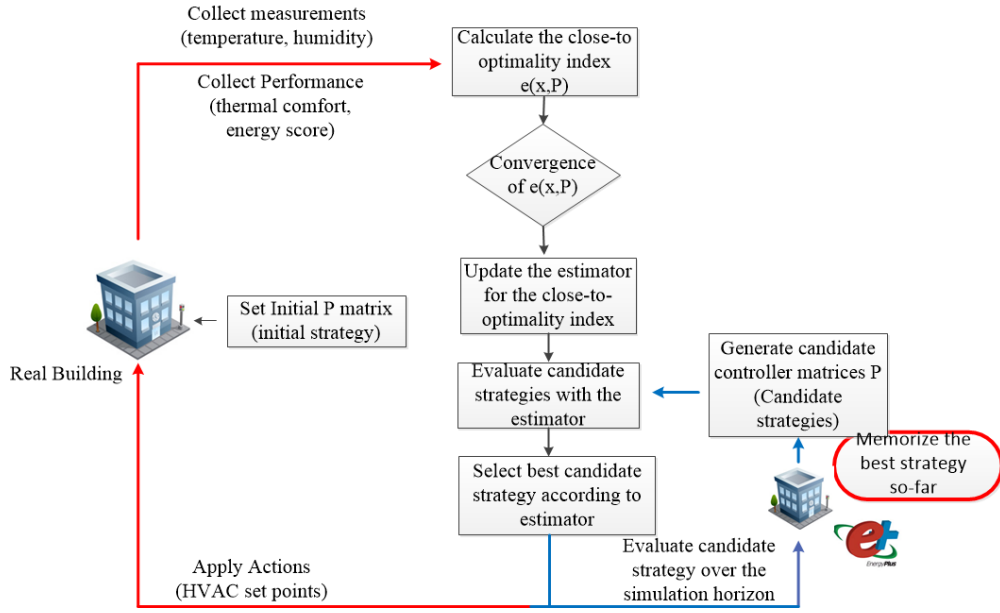


Figure 4: Local simulation-based optimization

4.3. Supervisory Logic

The purpose of this work is to provide a control architecture that be scalable to an arbitrary number N of buildings: for this reason, a centralized control architecture was discarded and the following bi-level supervisory strategy was implemented for the control and manipulation of each building/HVAC unit of the microgrid. The two levels can be identified as: a *local* building level and an *aggregate* microgrid level. In the simulations presented in this work three controllers, one for each building, operate using only local information plus information about weather forecast as we described in the sections above. At the aggregate level a supervisor takes into account the performance of each building and calculates the total cost, so as to optimize the global performance of the microgrid. As compared to a fully centralized strategy, the computational and communication requirements of the proposed control architecture are reduced. In Figure 5 the logic behind the supervisory strategy that we adopt is presented. In each building one local controller and one local optimization (PCAO Algorithm) is operated. The goal of each optimization algorithm is to optimize the performance of the building by taking into account only local information such as the thermal state of the building, occupancy information, and weather conditions. Each local controller communicates with the central node and offer information about the cost that the proposed control strategy is achieving and achieved in the past. The central node concentrates this information from each different building, calculates the total cost and decides if the ‘team’ of controllers achieved the best aggregate performance. The central node, informs the local levels with a binary signal, if the the best performance was achieved. Based on the Figure 4 the supervisory logic interacts only in the red circle (memorization of the best strategy). As a result, the update of the local controller is based on the best global performance rather than on the local performance. This simple strategy has been shown to be effective in achieving a good global performance: in particular, section V will show that, when a centralized architecture can be implemented, the performance of the centralized and of the proposed supervisory architecture (denoted as Supervisory PCAO) are comparable.

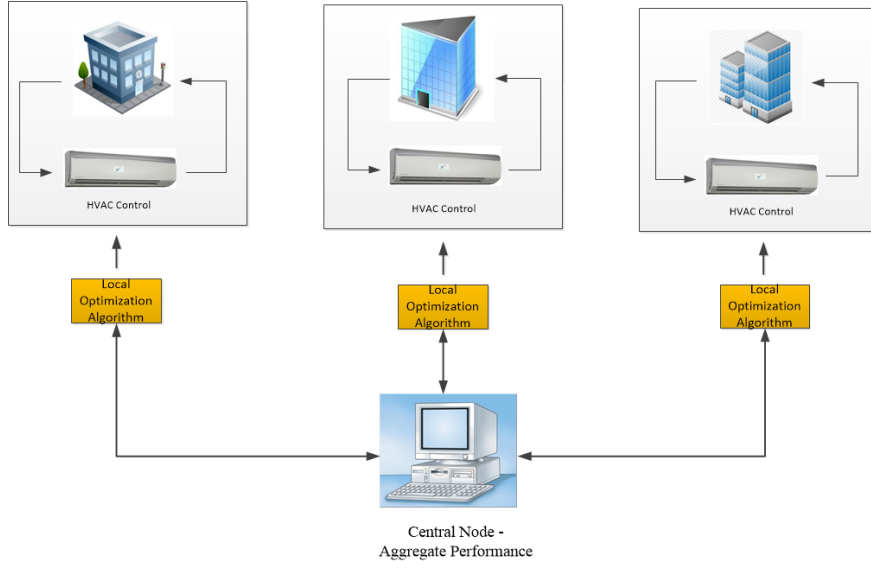


Figure 5: Supervisory control strategy

5. Simulation Results

This section describes the simulation results for the presented microgrid test case. The results of the optimization of the demand response and of the thermal comfort achieved via the Supervisory PCAO algorithm will be compared with the rule-based strategies $RBC_{24^{\circ}C}$ and $RBC_{25^{\circ}C}$, explained in section 3.2. Figure 6 shows the energy consumption and occupancy schedule under three control strategies ($RBC_{24^{\circ}C}$, $RBC_{25^{\circ}C}$ and PCAO). The distribution of solar and wind energy under the PCAO control strategy is also shown (the distribution of renewable energy under $RBC_{24^{\circ}C}$ and $RBC_{25^{\circ}C}$ is not shown for better readability of the plots). As mentioned, the renewable energy is distributed proportionally to the energy needs of each building. It can be noted how the PCAO algorithm is actively and dynamically managing the demand response side via HVAC regulation. It is interesting to note that the PCAO algorithm automatically implements the logic of the anticipating the use of HVAC devices some time before the arrival of people (the so-called pre-cooling effect). This action leads to the following intelligent behavior: in each building, the PCAO energy consumption rises about one hour before people arrive. This might look like a useless waste of energy, but it is not, because the comfort index in the PCAO case is relevantly improved over the two RBC scenarios. Since the control objective is the optimization of a combined criterion of energy pricing and thermal comfort, the overall the total cost is greatly reduced, as the following analysis will reveal.

Table 4: PCAO Improvement (Total Cost) with respect to $RBC_{24^{\circ}C}$ and $RBC_{25^{\circ}C}$ (results validated over 7 different sets of 3 days)

Case	Improvement wrt $RBC_{24^{\circ}C}$	Improvement wrt $RBC_{25^{\circ}C}$
Building 1	18-22%	12-17%
Building 2	15-19 %	10-15%
Building 3	19-22 %	13-16%
Microgrid	18-22 %	12-16%

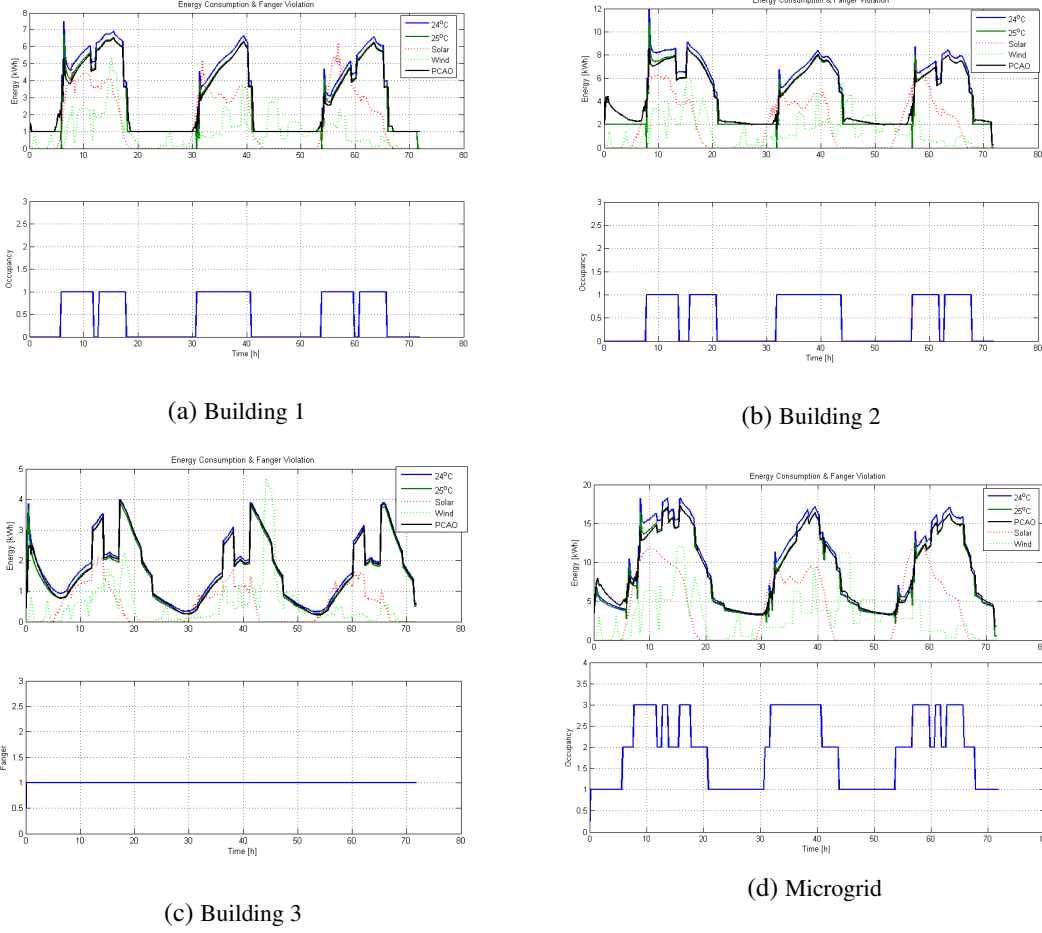


Figure 6: (a)-(b)-(c)-(d): Energy Consumption and Occupancy Schedule during the 3-days, for the three buildings and the whole microgrid test case

To evaluate the performance of the whole microgrid system and of its components, we calculate the total cost during the entire day. As we mentioned, the total cost consists of the energy cost and thermal comfort. Table 4 shows the improvement of PCAO with respect to the 2 rule-based controllers. In each case, the Supervisory PCAO strategy attains relevant improvements, ranging from 12 to 22% at the aggregate level. The variability arises from the different weather conditions: in fact, the results were validated over 7 different sets of 3 days, so as to show that the PCAO improvements are consistent in different environmental conditions (external temperature, humidity, solar radiation, and wind).

In Figure 7, the performance of each 3-day experiment is plotted with respect to energy cost (objective 1) and thermal comfort (objective 2). The figure proves that PCAO improvements are consistent in different conditions and different cases. Furthermore, the figure reveals that PCAO achieves better scores in both objectives: it is indeed remarkable to achieve a better thermal comfort while at the same time saving more energy. Mathematically, we say that the demand response strategy implemented by PCAO is Pareto optimal with respect to the demand response strategy implemented by the two RBCs. In fact, the solutions that PCAO offer are much closer to Utopia point than solutions of the other two demand response strategies. The Utopia point represents a solution that scores best in both objectives (Energy Cost and PPD), but that it

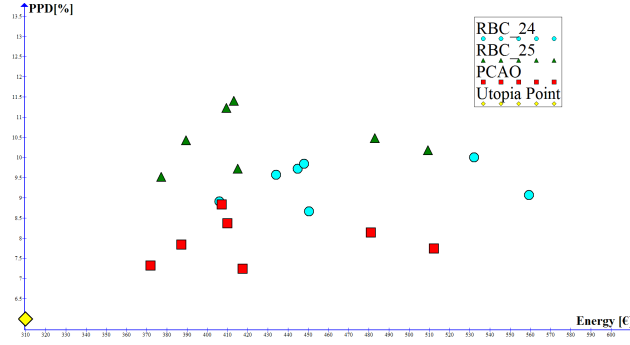


Figure 7: Energy cost (objective 1) and thermal comfort (objective 2) for 7 different experiments of 3 days: it is possible to notice that the 6 points on the extreme right represent very hot experiments where extra energy was required. The Utopia point represents an infeasible performance that cannot be achieved by any demand response strategy.

is impossible to reach.

To further investigate the PCAO improvements in comparison with the RBC scenarios, three more analyzes are presented, which are explained in the following sections.

5.1. Use of battery

The first analysis regards the use of battery: in Figure 8 and Table 5 the charging/discharging behavior of the battery is presented. Both $RBC_{25^{\circ}C}$ and PCAO algorithm perform better than $RBC_{24^{\circ}C}$. In fact, $RBC_{25^{\circ}C}$ and PCAO manage to charge the battery to a greater extent, so as to exploit this energy in the evening hours when no PV energy is available. Furthermore, PCAO outperforms $RBC_{25^{\circ}C}$, as it achieves to charge the battery a bit more and use for more time the energy. As a result, less energy from the main grid is absorbed, and PCAO manages to exploit better renewable energy resources and achieve better energy pricing. Table 5 shows to which extent the energy of the battery is better exploited: as compared with $RBC_{25^{\circ}C}$, it results that PCAO can exploit the battery for 2% more time (around half an hour every day), and the state of charge is on average 3% higher (around extra 70 kWh every day).

Table 5: Battery Information

Case	$RBC_{24^{\circ}C}$	$RBC_{25^{\circ}C}$	PCAO
Percentage of usage time	54%	61%	63%
Mean State of charge through experiment	15%	21%	24%

5.2. Participation of renewables

The second analysis regards the two histograms presented in Figure 9, which have been obtained from a 3-day simulation (one of the seven simulation presented above). The first histogram presents the energy cost in € for each building and the whole microgrid. The second histogram presents the mean percentage of people who are dissatisfied. As already revealed by Figure 7, PCAO achieves better scores in both histograms. In particular, with respect to $RBC_{24^{\circ}C}$, PCAO manages to save more than 50€ in 3 days for the whole system, while maintaining the comfort at better levels (2% better PPD score). On the other hand,

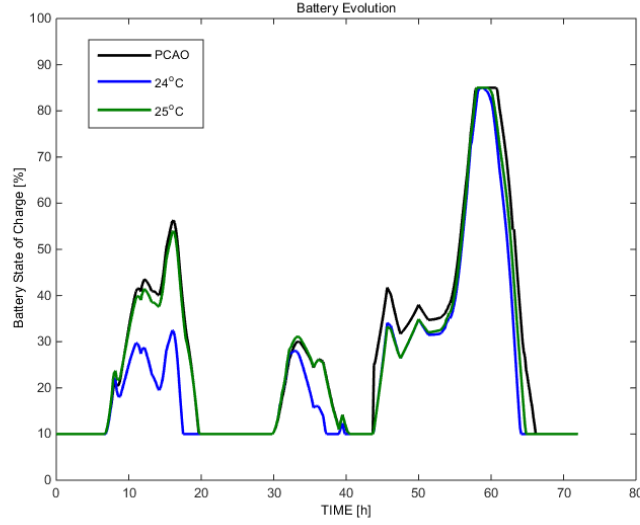


Figure 8: Battery evolution during the 3-day experiment

427 PCAO achieves a slightly better energy cost than $RBC_{25^{\circ}C}$: the energy cost is slightly better despite the pre-
 428 cooling effect implemented by PCAO that demands more energy consumption. Together with improving
 429 energy cost the PCAO strategy achieves a 3% improvement in PPD as compared with $RBC_{25^{\circ}C}$.

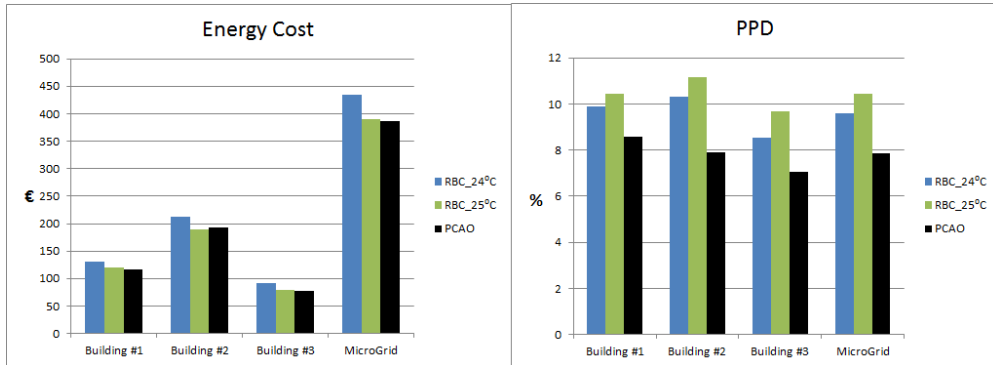


Figure 9: Energy Cost in Euros and Percentage of Dissatisfied People during the 3-day experiment.

430 It is also worth considering how the use of energy is divided among grid and renewable energy under the
 431 different demand response programs. Figure 10 shows that the percentage of renewable energy is higher in
 432 the PCAO case. Generally speaking, PCAO strategy achieves to exploit better renewable energy resources
 433 (and better battery usage), maintain better energy cost levels (even with precooling mode), but without
 434 sacrificing the comfort levels of users.

435 5.3. Robustness of solution-Sensitivity analysis

436 The final analysis is on robustness of the proposed solution: it is well known in control theory that
 437 a crucial requirement for the design of control strategies is their ability to perform in different conditions
 438 and show a certain level of robustness and tolerance with respect to changes of system conditions. More



Figure 10: Percentages of Renewable and Grid Energy

precisely, the above results were obtained from a control strategy that was optimized over a 3-day experiment. Thus, the resulting controller is optimized for the specific three days, with the specific occupancy schedule, weather conditions and needs: it is not clear how this controller might perform if tested in different days than the ones involved in the optimization step. That is why, in order to test the robustness of the proposed method, we tested the controller of the 3-day experiment, *in a 30-day experiment with different weather conditions and different occupancy schedules*.

Table 6: PCAO Improvement (Total Cost) with respect to $RBC_{24^{\circ}C}$ and $RBC_{25^{\circ}C}$ in a 30-day experiment

Case	Improvement wrt $RBC_{24^{\circ}C}$	Improvement wrt $RBC_{25^{\circ}C}$
Building 1	13-16%	8-11%
Building 2	11-14 %	7-9%
Building 3	16-19 %	10-13%
Microgrid	13-17 %	9-11%

In Table 6, the numerical results of the 30-day experiment are presented. Obviously, the improvements of Table 6, are slightly worse than the improvements of Table 4. However, the degradation of performance is acceptable, since the overall improvements range from 9 to 17% (as compared with 12-22% of Table 4). This means that a controller optimized over three days can be safely used over much longer horizons: the explanation for such a robustness lies in the feedback nature of the PCAO strategy: this is a clear advantage over, e.g. receding horizon based demand response programs that require the solution of an optimization problem at every time step.

5.4. Comparisons against a centralized architecture

As a final comparison, the proposed supervisory strategy is compared with a PCAO centralized strategy, proposed in [30], using information stemming from the entire microgrid.

In Table 7 the comparison between the two strategies is presented. The Centralized-PCAO strategy offers better performance than Supervisory-PCAO, but at the expense of slower convergence. It is to be

Table 7: Comparison (Total Cost) between supervisory and centralized PCAO strategy with respect to RBC_2 (results validated over 7 different sets of 3 days)

PCAO-Strategy	Improvement wrt RBC_2	Iterations
Supervisory	18-22 %	≈ 250
Centralized	22-26 %	≈ 550

expected that, with data stemming from the entire microgrid, the Centralized-PCAO is not scalable to microgrids with an increasing number of buildings. Thus, it is natural to raise concerns about its capability to be used in bigger problems, with more buildings (50-100). Moreover, as we mentioned earlier, in real cases, it is difficult to share private information as the energy-consumption or the demand response with a central node or with other partners. On the contrary, the proposed Supervisory strategy, minimize the exchange of information and rely heavily on the local optimization algorithms.

6. Conclusions

This paper presented a novel control algorithm for joint demand response management and thermal comfort optimization in a microgrid composed of three buildings, a photovoltaic array, a wind turbine, and an energy storage unit. The rationale for considering thermal comfort was that comfort plays a major role in dynamic demand response, especially in front of intermittent behavior of the renewable energy sources. The proposed control strategy adopted a two-level supervisory strategy: at the lower level, each building employed a local controller that processes only local measurements; at the upper level, a centralized unit supervised and updated the three controllers with the aim of minimizing the aggregate energy cost and thermal discomfort of the microgrid. Comparisons with alternative strategies revealed that the proposed supervisory strategy efficiently manages the demand response so as to sensibly improve independence of the microgrid with respect to the main grid, and guarantees (and improves) at the same time thermal comfort of the occupants. The renewable energy sources are fully exploited and better integrated with the main grid. Generally speaking, PCAO strategy achieves to exploit better renewable energy resources (and better battery usage), maintain better energy cost levels, but without sacrificing the comfort levels of users. The improvement are in the range of 12-22%: furthermore, the solution is robust as a controller optimized over 3 days can be used over much longer horizons (30 days) with improvements in the range 9-17%. Among the intelligent behaviors of the proposed strategy are: a pre-cooling action to avoid peaks of discomfort; modulation of the HVAC action to avoid peaks of energy consumption; better exploitation of energy from the battery; enhanced participation of renewable sources (and thus improved resilience from the grid and possibility to enable the islanded mode).

Acknowledgment

The research leading to these results has been partially funded by the European Commission FP7-ICT-2013.3.4, Advanced computing, embedded and control systems, under contract #611538 (LOCAL4GLOBAL).

References

- [1] Hassan Farhangi. The path of the smart grid. *Power and Energy Magazine, IEEE*, 8(1):18–28, 2010.

- [2] Nikos Hatziaargyriou, Hiroshi Asano, Reza Iravani, and Chris Marnay. Microgrids. *Power and Energy Magazine, IEEE*, 5(4): 78–94, 2007.
- [3] O Alsayegh, S Alhajraf, and H Albusairi. Grid-connected renewable energy source systems: challenges and proposed management schemes. *Energy Conversion and Management*, 51(8):1690–1693, 2010.
- [4] Robert L Fares and Michael E Webber. Combining a dynamic battery model with high-resolution smart grid data to assess microgrid islanding lifetime. *Applied Energy*, 137:482–489, 2015.
- [5] Ali Bidram and Ali Davoudi. Hierarchical structure of microgrids control system. *Smart Grid, IEEE Transactions on*, 3(4): 1963–1976, 2012.
- [6] Christopher O Adika and Lingfeng Wang. Smart charging and appliance scheduling approaches to demand side management. *International Journal of Electrical Power & Energy Systems*, 57:232–240, 2014.
- [7] Luis Pérez-Lombard, José Ortiz, and Christine Pout. A review on buildings energy consumption information. *Energy and buildings*, 40(3):394–398, 2008.
- [8] Liu Yang, Haiyan Yan, and Joseph C Lam. Thermal comfort and building energy consumption implications—a review. *Applied Energy*, 115:164–173, 2014.
- [9] ASHRAE. ANSI/ASHRAE standard 55-2004: thermal environmental conditions for human occupancy. *American Society of Heating, Refrigerating and air-Conditioning Engineers.*, 2004.
- [10] EU Commission et al. Renewable energy road map-renewable energies in the 21st century: building a more sustainable future. *COM (2006)*, 848, 2007.
- [11] EH Mathews, DC Arndt, CB Piani, and E Van Heerden. Developing cost efficient control strategies to ensure optimal energy use and sufficient indoor comfort. *Applied Energy*, 66(2):135–159, 2000.
- [12] Mingzhe Liu, Kim Bjarne Wittchen, and Per Kvols Heiselberg. Control strategies for intelligent glazed façade and their influence on energy and comfort performance of office buildings in denmark. *Applied Energy*, 145:43–51, 2015.
- [13] Zhu Wang, Rui Yang, Lingfeng Wang, RC Green, and Anastasios I Dounis. A fuzzy adaptive comfort temperature model with grey predictor for multi-agent control system of smart building. In *Evolutionary Computation (CEC), 2011 IEEE Congress on*, pages 728–735. IEEE, 2011.
- [14] M Mossolly, K Ghali, and N Ghaddar. Optimal control strategy for a multi-zone air conditioning system using a genetic algorithm. *Energy*, 34(1):58–66, 2009.
- [15] C Tzivanidis, KA Antonopoulos, and F Gioti. Numerical simulation of cooling energy consumption in connection with thermostat operation mode and comfort requirements for the athens buildings. *Applied Energy*, 88(8):2871–2884, 2011.
- [16] Frauke Oldewurtel, David Sturzenegger, and Manfred Morari. Importance of occupancy information for building climate control. *Applied Energy*, 101:521–532, 2013.
- [17] Xiaqi Xu, Patricia J Culligan, and John E Taylor. Energy saving alignment strategy: achieving energy efficiency in urban buildings by matching occupant temperature preferences with a buildings indoor thermal environment. *Applied Energy*, 123: 209–219, 2014.
- [18] Andrew Kusiak and Mingyang Li. Optimal decision making in ventilation control. *Energy*, 34(11):1835–1845, 2009.
- [19] Siddharth Goyal, Herbert A Ingley, and Prabir Barooah. Occupancy-based zone-climate control for energy-efficient buildings: Complexity vs. performance. *Applied Energy*, 106:209–221, 2013.
- [20] G. M. Kopanos, M. C. Georgiadis, and E. N. Pistikopoulos. Energy production planning of a network of micro combined heat and power generators. *Applied Energy*, 102:1522–1534, 2013.
- [21] Linfeng Zhang, Nicolae Gari, and Lawrence V Hmurcik. Energy management in a microgrid with distributed energy resources. *Energy Conversion and Management*, 78:297–305, 2014.
- [22] T. Broeer, J. Fuller, F. Tuffner, D. Chassin, and N. Djilali. Modeling framework and validation of a smart grid and demand response system for wind power integration. *Applied Energy*, 113:199–207, 2014.
- [23] JH Zheng, JJ Chen, QH Wu, and ZX Jing. Multi-objective optimization and decision making for power dispatch of a large-scale integrated energy system with distributed dhcs embedded. *Applied Energy*, 154:369–379, 2015.
- [24] Elizaveta Kuznetsova, Yan-Fu Li, Carlos Ruiz, and Enrico Zio. An integrated framework of agent-based modelling and robust optimization for microgrid energy management. *Applied Energy*, 129:70–88, 2014.
- [25] M. Marzband, A. Sumper, A. Ruiz-Alvarez, J. L. Dominguez-Garcia, and B. Tomoiaga. Experimental evaluation of a real time energy management system for stand-alone microgrids in day-ahead markets. *Applied Energy*, 106:365–376, 2013.
- [26] A. Parisio, E. Rikos, G. Tzamalís, and L. Glielmo. Use of model predictive control for experimental microgrid optimization. *Applied Energy*, 115:37–46, 2014.
- [27] Gabriele Comodi, Andrea Giantomassi, Marco Severini, Stefano Squartini, Francesco Ferracuti, Alessandro Fonti, Davide Nardi Cesarini, Matteo Morodo, and Fabio Polonara. Multi-apartment residential microgrid with electrical and thermal storage devices: Experimental analysis and simulation of energy management strategies. *Applied Energy*, 137:854–866, 2015.
- [28] Xiaohong Guan, Zhanbo Xu, and Qing-Shan Jia. Energy-efficient buildings facilitated by microgrid. *Smart Grid, IEEE*

- Transactions on*, 1(3):243–252, 2010.
- [29] NZ Azer and S Hsu. The prediction of thermal sensation from a simple model of human physiological regulatory response. *ASHRAE Trans*, 83(Pt 1), 1977.
 - [30] C. D. Korkas, S. Baldi, I. Michailidis, and E. B. Kosmatopoulos. Intelligent energy and thermal comfort management in grid-connected microgrids with heterogeneous occupancy schedule. *Applied Energy*, 149:194–203, 2015.
 - [31] Roberto Z Freire, Gustavo HC Oliveira, and Nathan Mendes. Predictive controllers for thermal comfort optimization and energy savings. *Energy and buildings*, 40(7):1353–1365, 2008.
 - [32] D Kolokotsa, A Pouliezios, G Stavrakakis, and C Lazos. Predictive control techniques for energy and indoor environmental quality management in buildings. *Building and Environment*, 44(9):1850–1863, 2009.
 - [33] Frauke Oldewurtel, Alessandra Parisio, Colin N Jones, Dimitrios Gyalistras, Markus Gwerder, Vanessa Stauch, Beat Lehmann, and Manfred Morari. Use of model predictive control and weather forecasts for energy efficient building climate control. *Energy and Buildings*, 45:15–27, 2012.
 - [34] Yudong Ma, Francesco Borrelli, Brandon Hancey, Brian Coffey, Sorin Bengea, and Philip Haves. Model predictive control for the operation of building cooling systems. *Control Systems Technology, IEEE Transactions on*, 20(3):796–803, 2012.
 - [35] Zhen Yu and Arthur Dexter. Simulation based predictive control of lowenergy building systems using two-stage optimization. *Proc. IBPSA09*, pages 1562–1568, 2009.
 - [36] Truong X Nghiem and George J Pappas. Receding-horizon supervisory control of green buildings. In *American Control Conference (ACC), 2011*, pages 4416–4421. IEEE, 2011.
 - [37] Carina Sagerschnig, Dimitrios Gyalistras, Axel Seerig, Samuel Prívarva, Jiří Cigler, and Zdenek Vana. Co-simulation for building controller development: The case study of a modern office building. In *Proc. CISBAT*, pages 14–16, 2011.
 - [38] Mousa Marzband, Majid Ghadimi, Andreas Sumper, and José Luis Domínguez-García. Experimental validation of a real-time energy management system using multi-period gravitational search algorithm for microgrids in islanded mode. *Applied Energy*, 128:164–174, 2014.
 - [39] Zhu Wang, Lingfeng Wang, Anastasios I Dounis, and Rui Yang. Multi-agent control system with information fusion based comfort model for smart buildings. *Applied Energy*, 99:247–254, 2012.
 - [40] D. B. Crawley, J. W. Hand, M. Kummert, and B. T. Griffith. Contrasting the capabilities of building energy performance simulation programs. *Building and environment*, 43(4):661–673, 2008.
 - [41] SA Klein. *TRNSYS: A transient simulation program*. Eng. Experiment Station, 1976.
 - [42] Ahmed Abdisalaam, Ioannis Lampropoulos, J Frunt, GPJ Verbong, and WL Kling. Assessing the economic benefits of flexible residential load participation in the dutch day-ahead auction and balancing market. In *European Energy Market (EEM), 2012 9th International Conference on the*, pages 1–8. IEEE, 2012.
 - [43] José Antonio Jardini, Carlos Tahan, MR Gouvea, Se Un Ahn, and FM Figueiredo. Daily load profiles for residential, commercial and industrial low voltage consumers. *Power Delivery, IEEE Transactions on*, 15(1):375–380, 2000.
 - [44] Imene Yahyaoui, Souhir Sallem, MBA Kamoun, and Fernando Tadeo. A proposal for off-grid photovoltaic systems with non-controllable loads using fuzzy logic. *Energy Conversion And Management*, 78:835–842, 2014.
 - [45] Cynthujah Vivekananthan, Yateendra Mishra, Gerard Ledwich, and Fangxing Li. Demand response for residential appliances via customer reward scheme. *IEEE Trans. Smart Grid*, 5(2):809–820, 2014.
 - [46] Wikipedia. Solar power, power cost. http://en.wikipedia.org/wiki/Solar_power#Power_cost, 2014.
 - [47] Wikipedia. Wind power, electricity costs and trends. http://en.wikipedia.org/wiki/Wind_power#Electricity_cost_and_trends, 2014.
 - [48] Noel Augustine, Sindhu Suresh, Prajakta Moghe, and Kashif Sheikh. Economic dispatch for a microgrid considering renewable energy cost functions. In *Innovative Smart Grid Technologies (ISGT), 2012 IEEE PES*, pages 1–7. IEEE, 2012.
 - [49] Kenichi Tanaka, Akihiro Yoza, Kazuki Ogimi, Atsushi Yona, Tomonobu Senjyu, Toshihisa Funabashi, and Chul-Hwan Kim. Optimal operation of dc smart house system by controllable loads based on smart grid topology. *Renewable Energy*, 39(1):132–139, 2012.
 - [50] Yang Peihong, Liu Wenying, and Wei Yili. A survey on problems in smart grid with large capacity wind farm interconnected. *Energy Procedia*, 17:776–782, 2012.
 - [51] Changsun Ahn, Chiao-Ting Li, and Huei Peng. Optimal decentralized charging control algorithm for electrified vehicles connected to smart grid. *Journal of Power Sources*, 196(23):10369–10379, 2011.
 - [52] David Lindley. Smart grids: The energy storage problem. *Nature*, 463(7277):18–20, 2010.
 - [53] Ioannis Hadjipaschalis, Andreas Poullikkas, and Venizelos Efthimiou. Overview of current and future energy storage technologies for electric power applications. *Renewable and Sustainable Energy Reviews*, 13(6):1513–1522, 2009.
 - [54] D. B. Crawley, L. K. Lawrie, F. C. Winkelmann, W. F. Buhl, Y. J. Huang, C. O. Pedersen, R. K. Strand, R. J. Liesen, D. E. Fisher, M. J. Witte, et al. Energyplus: creating a new-generation building energy simulation program. *Energy and Buildings*, 33(4):319–331, 2001.
 - [55] Richard Bellman and Robert E Kalaba. *Dynamic programming and modern control theory*. Academic Press New York, 1965.

- 600 [56] Simone Baldi, Iakovos Michailidis, Hossein Jula, Elias B Kosmatopoulos, and Petros A Ioannou. A plug-n-play computa-
601 tionally efficient approach for control design of large-scale nonlinear systems using co-simulation. In *Decision and Control*
602 *(CDC), 2013 IEEE 52nd Annual Conference on*, pages 436–441. IEEE, 2013.
- 603 [57] S. Baldi, I. Michailidis, E. B. Kosmatopoulos, and P. A. Ioannou. A plug and play computationally efficient approach for
604 control design of large-scale nonlinear systems using cosimulation. *IEEE Control Systems Magazine*, 34:56–71, 2014.
- 605 [58] I. Michailidis, S. Baldi, E. B. Kosmatopoulos, and P. A. Ioannou. Adaptive optimal control for large-scale non-linear systems.
606 *IEEE Transactions of Automatic Control*, page under review, 2014.